

Final-state screening effect in the 3s photoemission spectra of Mn and Fe insulating compounds

Gey-Hong Gweon, Je-Geun Park, and S.-J. Oh

Department of Physics, Seoul National University, Seoul 151-742, Korea

(Received 11 March 1993)

The satellite structures of 3s core-level photoemission spectra of Mn and Fe dihalides and mono-oxides have been studied systematically. We found that exchange splitting between 3s holes and 3d electrons, intrashell electron correlation, and final-state screening (charge-transfer satellite) effects all contribute to their satellite structures. We extended the existing model of 2p core-hole satellite structures for transition-metal compounds [Park *et al.*, Phys. Rev. B **37**, 10 867 (1988)] to the case of 3s core holes by including the exchange interaction and the intrashell electron correlation effect. The intrashell electron correlation effect is included by introducing two parameters, the energy separation and the coupling strength between $\underline{3s}3d^n$ and $\underline{3p}^23d^{n+1}$ states. With this model, we were able to explain very well the 3s spectra of the Mn and Fe insulating compounds studied here, and which were consistent with their 2p core-level spectra analyses. We observe that the importance of final-state screening effects in the core-level spectra depends on the ligands. As a result, 3s energy splittings for very ionic compounds such as MnF₂ and FeF₂ can be well understood by exchange splitting alone, but that 3s splittings in other compounds in general are not directly related to the 3d local magnetic moment of the ground state. We found that the change of 3s splittings in more covalent compounds is mostly determined by the final-state screening due to the different values of 3s-hole-3d-electron Coulomb attraction Q depending upon the spin of the final state, rather than the exchange energy between 3s holes and 3d electrons.

I. INTRODUCTION

The satellite structures in the 3s core-level photoemission spectra of Mn and Fe compounds have received much attention,¹⁻⁷ and have been the subject of controversy for some time. The basic concept underlying the 3s photoemission is the Van Vleck theorem,⁸ which states that the configuration s^l^n , obtained by removing one s electron from the s^2l^n configuration with total spin $S(>0)$, has two multiplet terms of spin $S \pm \frac{1}{2}$ with energy separation

$$\Delta E = \frac{2S+1}{2l+1} G^l(s,l),$$

where $G^l(s,l)$ is the Slater exchange integral and $l=2$ for an unfilled d shell. Evaluating ΔE using the final state $G^l(s,l)$ value is sometimes called the multiplet-hole theory and we will follow this terminology. This simple atomic interpretation is quite appealing in that the experimentally determined peak separation can be used to determine the magnetic moment due to unpaired 3d electron spins in the solid. However, some discrepancies between this theory and experiment were observed such as the fact that the measured separation is usually a factor of 2 smaller than predicted by free-atom exchange integral calculations and that the intensity ratio deviates from the multiplicity ratio.^{1,9,10} Bagus, Freeman, and Sasaki² noted that the 2s peak splitting was reasonably predicted by the multiplet-hole theory in contrast to 3s peak splitting in MnF₂, so they included an intrashell correlation effect into the simple multiplet theory by considering excitations such as $\underline{3s}3d^n \rightarrow \underline{3p}^23d^{n+1}$ or $\underline{3s}3d^n \rightarrow \underline{3s}3p^23d^{n+2}$ in the 3s photoemission final state. This way they were able to obtain far better agreement

between theory and experiment and showed clearly how the intrashell correlation effect in the final state reduces both the energy separation and the intensity ratio of main and satellite peaks in MnF₂. This interpretation was not restricted to Mn²⁺ and similar multiconfigurational Hartree-Fock calculations were performed¹¹ for Fe²⁺, Fe³⁺, ..., Ni²⁺. It seems to be generally accepted that this intrashell correlation causes the reduction of the observed energy splittings. For most of the transition-metal fluorides or oxides, 3s splitting is close to half the multiplet-hole theory value.¹⁰ With these understandings, even a calibration curve has been proposed for Mn and Fe compounds,¹² and this curve was used to "determine" the local magnetic moment of several Fe intermetallic compounds.^{13,14}

However, this interpretation is not complete in that it does not properly take into consideration the effect of core-hole screening in the final state of photoemission. Final-state screening effects in the 2p core-level spectra of transition-metal compounds has been studied extensively.¹⁵⁻¹⁸ The main point is that the Coulomb attraction between the core-hole and localized 3d electrons is so strong that in some compounds the main peak at lower binding energy corresponds to the final eigenstate with one more 3d electron than the ground-state configuration. When this is the case, there exist strong satellites at the higher binding-energy side, which are called "charge-transfer satellites." The intensity and energy position of this charge-transfer satellite depends on the electronegativity of the ligand through the quantity called "charge-transfer energy" Δ . This quantity, together with d - d Coulomb energy U , provides a model which gives a sound understanding of electronic properties of many transition-metal compounds,¹⁹ complementing the

original Mott-Hubbard theory. For example, the band gaps of FeO, CoO, and NiO can be calculated from the parameters obtained in the analyses of their $2p$ core-level satellite structures,¹⁸ and they show good agreement with experiments.

The interpretation of $3s$ core-level spectra taking into account the final-state screening effect was first proposed by Veal and Paulikas.³ They proposed, based on their atomic calculations, that the main peak in the $3s$ core-level spectra corresponds to the "locally screened" state with one extra $3d$ electron. They therefore claimed that the $3s$ splitting is mostly determined by the exchange interaction in the $3d^{n+1}$ configuration rather than the ground-state $3d^n$ configuration. This model of local screening for the $3s$ core hole is not free from disputes, however. The magnitude of $3s$ splitting as a function of the d -electron number seems to favor the $3d^n$ final-state configuration,²⁰ and the experiment on gas-phase Mn⁵ shows Mn $3s$ and $3p$ spectra quite similar to those of MnF₂ and MnO. The spin-polarized photoelectron diffraction patterns also seem consistent with "unscreened" $3s$ final states.⁴ This question of screening along with the recent study⁶ which shows poor correlation between Fe $3s$ splittings and magnetic moments in many Fe compounds renders the original interpretation of exchange-split satellites questionable.

So, we have a question which is crucial for the proper understanding of the $3s$ spectra: How important is final-state screening for $3s$ core-level spectra? The answer to this question will settle the disputes about the origin of $3s$ satellites and their relevance to the local magnetic moments in $3d$ transition-metal insulating compounds. Here, we tried to answer this question by systematically studying Mn and Fe dihalide series MnF₂, MnCl₂, MnBr₂, FeF₂, FeCl₂, FeBr₂, and mono-oxides MnO and FeO. The basic ideas behind this study are the following. First, the final-state screening effect in the core-level spectra depends strongly on the electronegativity of the anion.¹⁵⁻¹⁷ However, most studies to date^{1,3,4,5,20} are restricted to very ionic compounds such as fluorides and oxides. By studying chlorides and bromides, we can complement these data and get the whole picture. Second, the interpretation of $3s$ core-level spectra should be consistent with that of the $2p$ spectra. In fact, the $2p$ core-level spectra of Mn and Fe dihalide compounds including peak separations and their intensity ratios have been well understood with charge-transfer model and the relevant parameters were determined already.^{17,18} In this study we extended this model to the $3s$ spectra and tried to interpret both $2p$ and $3s$ spectra consistently by using the same model parameters.

In the interpretation of the $3s$ spectra we assumed a different amount of Coulomb interaction between the core-hole and $3d$ electrons in the high-spin and low-spin final states with a $3s$ hole. And to include the intrashell correlation effect of Bagus, Freeman, and Sasaki,² we introduced two parameters, the energy separation and the coupling strength between $3s3d^n$ and $3p^23d^{n+1}$, which were adjusted to fit the experimental spectra. We found that all the spectra studied here are explained very well within our model with reasonable parameters, and con-

sistently with the $2p$ spectra. We found that, as in the $2p$ case, the character of the $3s$ main peaks changes depending on the ligand. For fluoride, they are "unscreened" peaks, whereas they are "locally screened peaks" for bromides. Main peaks for chlorides (and oxides to a less extent) are of mixed character. This finding is a contradiction to the proposal of Veal and Paulikas. Also, because of the final-state screening mechanism present, we see that the peak which has been assigned simply as an exchange-split low-spin peak is, in fact, a composite peak consisting of a low-spin main peak and a high-spin charge-transfer peak for many compounds. So when the final-state screening effect becomes strong, we can no longer assign the experimentally observed peak separation as the exchange splitting. Furthermore, the energy separation between the high-spin main peak and the low-spin main peak is affected by the screening. This effect, resulting from the stronger screening in the low-spin final state rather than in the high-spin final state because of different Q values, tends to reduce the energy splitting compared with that expected from the simple Van Vleck theorem. These effects explain why the actual experimental $3s$ splittings show poor correlation with the local magnetic moments in many insulating Fe compounds as reported in Ref. 6.

The organization of this paper is as follows. We describe samples and experimental details in Sec. II. We introduce our model which considers exchange interaction, intrashell correlation effect, and charge-transfer model on an equal footing in Sec. III. In Sec. IV analyses are made on the experimental spectra, and in Sec. V we discuss the final-state screening effect on the $3s$ spectra. A brief summary of our results on dihalides has been published previously.²¹ Here, we will present complete details and also include analyses on mono-oxides.

II. EXPERIMENT

The dihalide samples were all obtained commercially (Johnson Matthey Co.) in powder form. They were all anhydrous and the purities were 97–99.999%. They were pressed into pellets under 200 kg/cm² pressure and were baked in a vacuum oven for several hours at about 150°C (except for MnCl₂ and MnBr₂) before being introduced into the x-ray photoemission spectroscopy (XPS) spectrometer chamber made by VSW Scientific Instruments in England. MnCl₂ and MnBr₂ were baked in a vacuum oven for more than 12 h at a temperature of 50°C–55°C because they are known to have melting points near 60°C. These dihalide samples were scraped *in situ* with a diamond file just before the experiment until carbon and oxygen contaminations became negligible. The FeO sample was a single crystal which was fractured to get a fresh surface. The pressure in the analysis chamber was maintained below 1×10^{-9} mbar, except for MnCl₂ and MnBr₂ where only $\sim 1 \times 10^{-8}$ mbar could be maintained because of outgassing. The photon source was the Mg $K\alpha$ line (1253.6 eV) for FeCl₂, FeBr₂, MnBr₂ ($3s$), and the Al $K\alpha$ line (1486.6 eV) for FeF₂, FeO, MnF₂, MnCl₂, MnBr₂ ($2p$). One thing worth commenting on is that we had to use only the Mg $K\alpha$ source to take Mn or

Fe 3s spectra of bromides because Br Auger lines as strong as Fe or Mn 3s peaks appear in the very near region of the 3s spectra when we used Al $K\alpha$ as the photon source. The concentric hemispherical electron-energy analyzer was used with the pass energy of 44 eV, which resulted in the overall spectrometer resolution (photon source and the analyzer) of ~ 1.2 eV full width at half maximum (FWHM).

III. CHARGE-TRANSFER MODEL AND INTRASHELL CORRELATION

The charge-transfer model in its cluster approximation and its relevance to the more fundamental Anderson impurity model is described in detail elsewhere.¹⁵⁻¹⁷ Here, we will use the theory developed in Ref. 17. Although there was slight improvement of the theory¹⁸ by including the anisotropy of hybridization T between the metal d electron and ligand p electron, this is not at all a crucial ingredient of the model and the main result of this inclusion of the crystal-field effect is just the slight change of the T values. So, we will ignore this consideration here for simplicity. Also, we will ignore the energy difference of t_{2g} and e_g orbitals as it has been shown to be a safe procedure in this case.¹⁸ For all the materials we studied here, the local cluster MX_6 , where M is a transition-metal ion and X is a halide or oxygen ion, is an octahedron.²²

To introduce the intrashell correlation model proposed to interpret the 3s spectra of fluorides and oxides into the frame of this charge-transfer model, we present a simplified simulation of that model. Results of the multiconfigurational Hartree-Fock calculations^{2,11} show that the high-spin final state (6S for Mn^{2+} and 7D for Fe^{2+}) is essentially unaffected by the correlation effect. On the other hand, the low-spin final state (4S for Mn^{2+} and 5D for Fe^{2+}) is strongly affected by the correlation effect because in this case there are many low-lying states available to which the $3s3d^n$ configuration can be excited. So, we will assume here that the high-spin final state is not affected by the intrashell correlation effect, and use the same final-state Hamiltonian as in the case of $2p$ core-level analysis. For low-spin final states, the excitations considered in previous studies are of the type $3s3d^n \rightarrow 3p^23d^{n+1}$ or $3s3d^n \rightarrow 3s3p^23d^{n+2}$ with the excitation energies ~ 10 and ~ 100 eV, respectively.² We will consider only the former type of excitations, because the excitation energy of the latter is very large. Actually there is more than one multiplet state that can be obtained by the excitation $3s3d^n \rightarrow 3p^23d^{n+1}$. However, we will make a simplified simulation by considering only one excited state $3p^23d^{n+1}$ for the $3s3d^n$ state in the low-spin final state of photoemission. The energy separation E_{ic} and the coupling strength V_{ic} of these two states are adjusted to fit the experimental spectra. The next (and final) step of our modelization of the 3s spectroscopy is to consider the charge-transferred states of $3p^23d^{n+1}$ just as we consider those of the $3s3d^n$ state.

So, in the low-spin final-state Hamiltonian with a 3s hole we consider states of the type $3p^23d^{n+q+1}\underline{L}^q$ that couple to the $3s3d^{n+q}\underline{L}^q$ states ($q=0,1,\dots,9-n$), while in the high-spin final-state Hamiltonian with a 3s

hole or in the $2p$ hole final-state Hamiltonian only the latter type of states (charge-transfer type) are considered. Values of n are 5 for Mn^{2+} and 6 for Fe^{2+} . The dimension of the Hamiltonian matrix in the 3s low-spin case is $2(10-n)+1$ compared with $10-n+1$ for the 3s high-spin or $2p$ final states. The Hamiltonian matrix elements of our model for the 3s core-hole low-spin final state have the following forms:

$$\begin{aligned} \langle 3s3d^n | H | 3s3d^n \rangle &= E_{MHT}, \\ \langle 3s3d^{n+1}\underline{L} | H | 3s3d^{n+1}\underline{L} \rangle &= E_{MHT} + \Delta - Q_L, \\ \langle 3s3d^{n+2}\underline{L}^2 | H | 3s3d^{n+2}\underline{L}^2 \rangle &= E_{MHT} + 2(\Delta - Q_L) + U, \\ \langle 3p^23d^{n+1} | H | 3p^23d^{n+1} \rangle &= E_{MHT} + E_{ic}, \\ \langle 3p^23d^{n+2}\underline{L} | H | 3p^23d^{n+2}\underline{L} \rangle &= E_{MHT} + E_{ic} \\ &\quad + (\Delta - 2Q_{3p} + u) + U, \\ \langle 3p^23d^{n+3}\underline{L}^2 | H | 3p^23d^{n+3}\underline{L}^2 \rangle &= E_{MHT} + E_{ic} \\ &\quad + 2(\Delta - 2Q_{3p} + u) + 3U, \\ \langle 3s3d^n | H | 3s3d^{n+1}\underline{L} \rangle &= \sqrt{10-n} T, \\ \langle 3s3d^{n+1}\underline{L} | H | 3s3d^{n+2}\underline{L}^2 \rangle &= \sqrt{2(9-n)} T, \\ \langle 3s3d^{n+2}\underline{L}^2 | H | 3s3d^{n+3}\underline{L}^3 \rangle &= \sqrt{3(8-n)} T, \\ \langle 3p^33d^{n+1} | H | 3p^33d^{n+2}\underline{L} \rangle &= \sqrt{(9-n)} T, \\ \langle 3p^23d^{n+2}\underline{L} | H | 3p^23d^{n+3}\underline{L}^2 \rangle &= \sqrt{2(8-n)} T, \\ \langle 3s3d^{n+q}\underline{L}^q | H | 3p^23d^{n+q+1}\underline{L}^q \rangle &= V_{ic}, \end{aligned}$$

$(q=0,1,\dots,9-n).$

Here, our reference energy is the energy of the $3s3d^n$ high-spin final configuration and E_{MHT} is the energy separation given by the multiplet-hole theory. Δ is the charge-transfer energy from the ligand to transition-metal ion, U is the $d-d$ Coulomb interaction, Q is the Coulomb interaction between the core hole and d electron, u is the Coulomb interaction between the ligand hole and d electron, and T is the hybridization parameter between the ligand p orbital and the transition-metal d orbital. E_{ic} and V_{ic} were introduced above. If we just discard the states connected by E_{ic} and V_{ic} , then this Hamiltonian reduces to the 3s high-spin or the $2p$ final-state Hamiltonian. Since Δ , U , u , and T are parameters related to valence electronic structures, we expect them to essentially be the same in both $2p$ and $3s$ core-hole cases. However, Q is the Coulomb interaction energy between the core hole and d electron, so we expect its value to change depending on the core hole. We will denote Q_L as the 3s hole d -electron Coulomb attraction in the 3s low-spin final state, and Q_H as that in the high-spin final state. Q_{2p} (Q_{3p}) is the Coulomb attraction between the d electron and $2p$ ($3p$) hole.

We must make clear at this point that charge-transfer parameters Δ , U , and Q are not atomic parameters but are renormalized from atomic values by the polarization correction (E_p), Madelung correction (E_M), core hole-ligand hole repulsion (q), or d -electron ligand-hole in-

teraction (u).¹⁶ For example, Q is defined as

$$Q = Q_0 - 2E_p - q,$$

$$Q_0 = \langle cd^n | H | cd^n \rangle - \langle cd^{n+1} | H | cd^{n+1} \rangle$$

$$- [\langle d^n | H | d^n \rangle - \langle d^{n+1} | H | d^{n+1} \rangle].$$

This is the reason why u appears in the diagonal elements of the Hamiltonian above. We assumed $q = u$ in writing the Hamiltonian to reduce the number of parameters. On the other hand, E_{MHT} , E_{ic} , and V_{ic} are atomic parameters by definition. Also, the energy difference between $3s3d^{n+q}\underline{L}^q$ and $3p^23d^{n+q+1}\underline{L}^q$ must be atomic values. This can be easily checked as, for example,

$$\langle 3p^23d^{n+2}\underline{L} | H | 3p^23d^{n+2}\underline{L} \rangle$$

$$- \langle 3s3d^{n+1}\underline{L} | H | 3s3d^{n+1}\underline{L} \rangle = Q_{L0} - 2Q_{3p0} + U_0,$$

where the subscript 0 means atomic value.

The initial (ground) state Hamiltonian can be obtained as usual by setting $Q = 0$ in the $2p$ (or $3s$ high spin) final-state Hamiltonian. The energy of positions of various photoemission peaks are given by the eigenvalues of the final-state Hamiltonian, and their intensities are given by the overlap between the final eigenstate and the lowest initial eigenstate by the sudden approximation.

IV. ANALYSIS OF THE SPECTRA

A. $2p_{3/2}$ spectra of dihalides

We analyzed the $2p_{3/2}$ spectrum as in previous papers.¹⁶⁻¹⁸ In Figs. 1 and 2 we show the $2p_{3/2}$ spectra of Mn and Fe dihalides with fitting curves. The inelastic background and x-ray source satellites have been subtracted from the raw data. The multiplet structures of the $2p_{3/2}$ final states are known to give rise to an asymmetric line shape of the main peaks,²³ but we have ignored them here and fitted the peaks with one or two broad Gaussians. That is why the peak positions of the fitting curves are generally displaced to the high binding-energy side by about 0.5 eV compared with the experimental data. The fitting curves shown in Fig. 1 are the best fit we found using the Hamiltonian described in Sec. III. The model parameters obtained in the least-square fits are listed in the first four columns of Table I. These model parameter values are practically equal to those obtained in Ref. 17. We note that in fluorides Δ is larger than Q_{2p} , hence the main peak is mostly of the d^n configuration corresponding to the "unscreened peak." On the other hand, in bromides Δ becomes smaller than Q_{2p} , which results in the main peak with largely d^{n+1} configuration corresponding to the "locally screened" peak. Hence, we see that the degree of extra atomic relaxation contributions to the $2p$ core-level spectra depends strongly on the charge-transfer energy Δ , which is determined by the electronegativity of the ligand.

B. $3s$ spectra of dihalides

In Figs. 3 and 4 we show the $3s$ spectra of Mn and Fe dihalides, respectively. X-ray source satellites and the inelastic electron background have been subtracted from the raw data, except for the case of bromides where plasmon satellites of the Br $3d$ peak strongly superimpose Mn $3s$ and Fe $3s$ peaks. The $3s$ spectra on MnF_2 , FeF_2 , and FeCl_2 are consistent with those published earlier,^{1,24} and those on MnCl_2 , MnBr_2 , FeBr_2 have not been reported in the literature to our knowledge. The extra broadening found in our MnF_2 $3s$ spectrum probably comes from some instability of our experiments. However, the energy separation and the intensity ratio we obtained from the fitting were similar to those reported previously in the literature.^{1,2} We first note that MnCl_2 and FeCl_2 have three peak structures instead of two, which is contrary to the expectation of the simple exchange splitting. One can

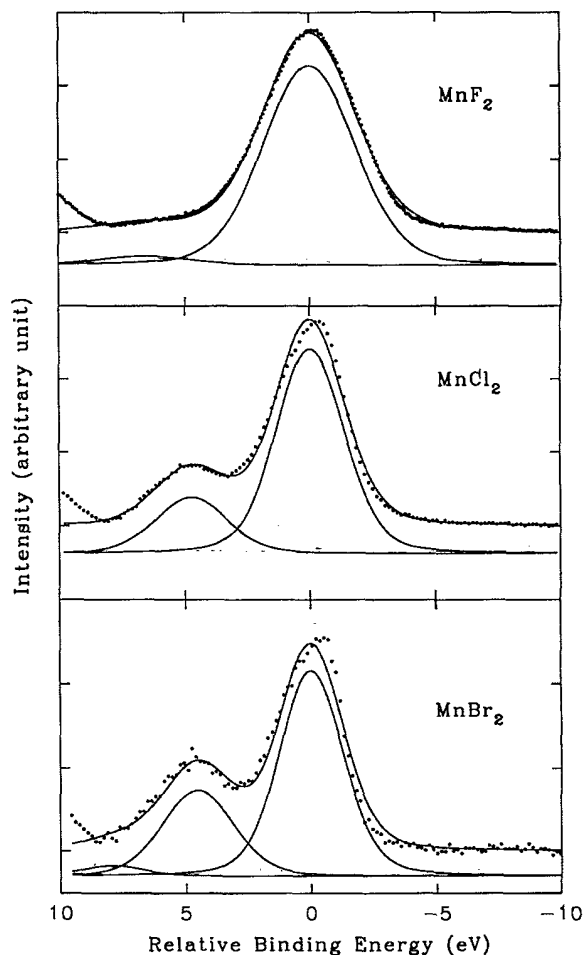


FIG. 1. The $2p_{3/2}$ spectra of Mn dihalides. Inelastic background and x-ray source satellites were subtracted from the raw data. Fitting curves and their component peaks are shown. Lorentzian width (FWHM in eV) was fixed at 0.7. Gaussian widths (FWHM in eV) are 3.9 for MnF_2 , 2.8 for MnCl_2 main peak, 3.0 for MnCl_2 satellite, 2.6 for MnBr_2 main peak, and 3.0 for MnBr_2 satellites. (For MnBr_2 the Gaussian width for two satellites were constrained to be equal.)

TABLE I. The model Hamiltonian parameter values (in units of eV) and the estimated ground-state d -electron numbers $\langle n_d \rangle_{\text{ini}}$ of cations obtained from the fit of $2p_{3/2}$ and $3s$ core-level spectra for Mn and Fe dihalides and mono-oxides.

	Δ	U	T	Q_{2p}	Q_H	Q_L	Q_{3p}	E_{ic}	V_{ic}	$\langle n_d \rangle_{\text{ini}}$
MnF ₂	10.0	3.4	1.3	4.9	3.3	4.8	3.9	14.6	13.2	5.08
MnCl ₂	5.6	3.4	1.3	4.9	3.3	4.8	3.9	14.6	13.2	5.20
MnBr ₂	3.8	3.3	1.2	4.7	3.3	4.8	3.9	14.6	13.2	5.30
FeF ₂	9.2	4.0	1.5	5.7	4.5	5.8	5.0	12.5	10.8	6.09
FeCl ₂	5.2	4.0	1.4	5.7	4.5	5.8	5.0	12.5	10.8	6.21
FeBr ₂	3.6	3.9	1.3	5.6	4.5	5.8	5.0	12.5	10.8	6.30
MnO	7.4	3.2	1.5	4.6	3.3	4.8	3.9	14.6	13.2	5.17
FeO	6.5	3.9	1.5	5.6	4.5	5.8	5.0	12.5	10.8	6.17

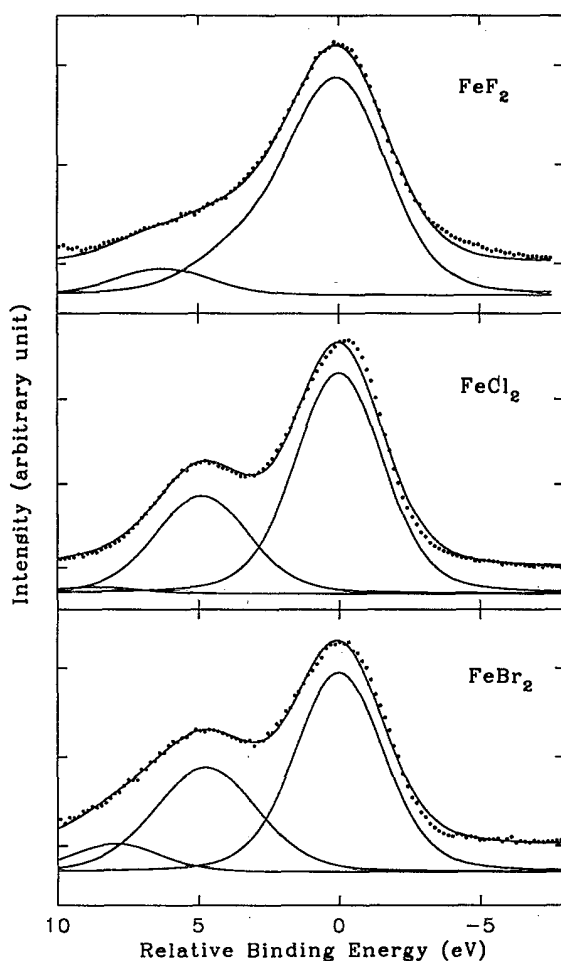


FIG. 2. The $2p_{3/2}$ spectra of Fe dihalides. Inelastic background and x-ray source satellites were subtracted from the raw data. Fitting curves and their component peaks are shown. Lorentzian width (FWHM in eV) was fixed at 0.9. Gaussian widths (FWHM in eV) are 3.6 for FeF₂, 3.2 for FeCl₂ main peak, 3.4 for FeCl₂ satellite, 3.2 for FeBr₂ main peak, and 3.8 for FeBr₂ satellites. (For FeBr₂ the Gaussian width for two satellites were constrained to be equal.) For FeF₂ the main peak shown actually consists of two peaks separated by 3.4 eV and intensity ratio 1:0.2, which was necessary to fit the asymmetric shape due to multiplets.

think of an intrashell correlation effect as a possible origin of these additional peaks, but we discard this possibility for two reasons. First, for Mn²⁺ and Fe²⁺ ions the satellites originating from this electron correlation effect have been calculated, and are shown to be more than 20 eV away from the main peak.^{2,11} Second, the intensity of the second peak in the FeCl₂ 3s spectra, which we obtained from fitting the spectra simply with three peaks, is about 75% of the main (first) peak, which is larger than 67% expected from the multiplicity ratio. This is contrary to what is expected of the electron correlation effect,¹¹ which tends to *reduce* the exchange satellite intensity. Hence, an additional mechanism is called for to explain these satellite structures besides exchange splitting and intrashell correlation effect.

An obvious candidate for this additional mechanism is the charge-transfer satellite arising from the extra-atomic relaxation of the 3s core hole. To prove this conjecture, we performed the model calculation that is described fully in Sec. III. The values for E_{MHT} are taken from the theoretical calculation,¹¹ which gives 14.3 eV for Mn²⁺ and 12.4 eV for the Fe²⁺ ion. The parameters of intrashell correlation effect E_{ic} and V_{ic} are assumed to be the same for a given ion, and are adjusted to fit the experimental data. The values we used are given in Table I. We now see if we can fit the experimental 3s spectra by choosing appropriate parameters of the model, which are consistent with those obtained from the 2p core-level analysis above. For this purpose, we used the same values of the charge-transfer model parameters used in the 2p analysis except for Q values. We checked the changes of U and Q using the optimized orbital Hartree-Fock atomic calculation. We found that U_0 changes by only ~ 0.5 eV in going from the 2p core hole to 3s core hole. The change of Q_0 was substantial. Calculated values are $Q_{2p0}^{\text{ave}} = 17.1$ eV, $Q_{H0} = 14.4$ eV, $Q_{L0} = 17.6$ eV for Mn²⁺, and 18.2, 15.5, 18.6 eV, respectively, for Fe²⁺. Intuitively, the change of Q value will be the primary effect, since U and T are sort of the average between initial-state and final-state values while Q is definitely a final-state parameter. So we will assume that the parameters except Q will not be changed in going from 2p core hole to 3s core hole. Since the amount of renormalization due to the solid-state effect¹⁶ should be largely independent of the core-hole orbital, we can say that the difference found in the

Q_0 values will be reflected in the actual charge-transfer model parameters. Therefore, we expect that Q_L will be nearly equal to Q_{2p} while Q_H will be smaller by a few eV. We further assume that Q_{3p} is equal to the multiplicity weighted average of Q_H and Q_L to reduce the number of free parameters.

In this spirit, we have fitted the 3s spectra of MnF_2 , FeF_2 , MnCl_2 , and FeCl_2 as shown by the solid lines in Figs. 3 and 4. The values of Q_H and Q_L used in these fits are listed in Table I. The intrashell correlation parameters E_{ic} and V_{ic} were both found to be ~ 10 eV, which is consistent with multiconfigurational Hartree-Fock calculation.² We also need the ligand-hole d -electron Coulomb interaction u in the calculation of 3s final-state Hamiltonian eigenstates, and this was estimated by the point-charge approximation in the dielectric medium as was done before.^{16,18} The electronic dielectric constant

was estimated using the Clausius-Mossotti relation, and the atomic polarizability of cations²⁵ and anions²⁶ were taken from published data. In Table II we show u values along with cation-anion distances²² and the electronic dielectric constants ϵ_∞ . We see in Figs. 3 and 4 that the fits reproduce the experimental data very well, with the parameter values which are all consistent with the above assumptions. The only discrepancy may be the separation between Q_L and Q_H which is about half of the expected value from the atomic calculation. We think this comes from the crudeness of our model, especially concerning the intrashell correlation effect. In modeling the intrashell correlation effect, we assumed same coupling strength between the states $3p^2 3d^{n+q+1} \underline{L}^q$ and $3s 3d^{n+q} \underline{L}^q$ independently of q ($0, 1, \dots, 9-n$). It seems likely that this coupling strength is not constant for all values of q but rather a decreasing function of q . This

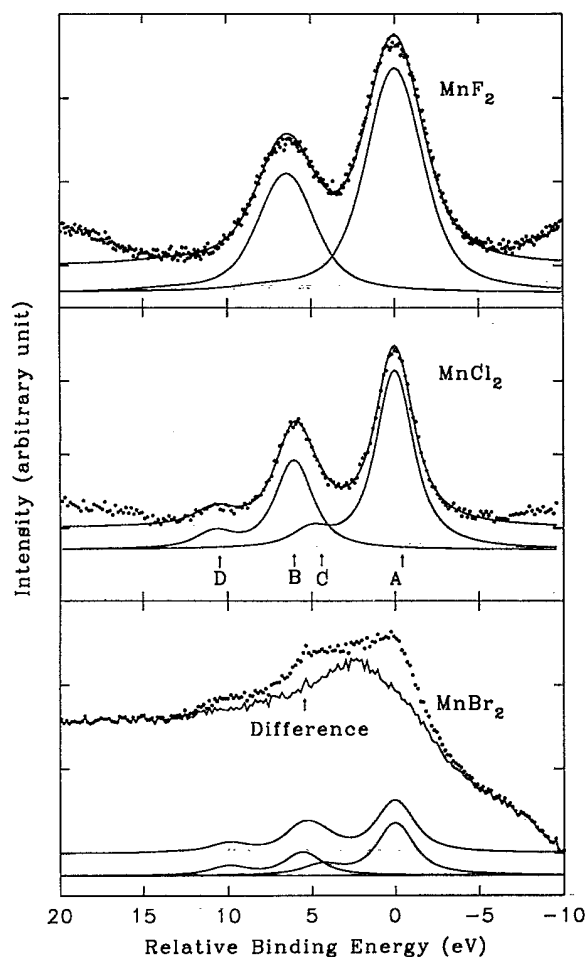


FIG. 3. The 3s spectra of Mn dihalides. Inelastic background and x-ray source satellites were subtracted from the raw data, except for the case of MnBr_2 where only x-ray source satellites were subtracted. Fitting curves and their components are shown. Gaussian width (FWHM in eV) was fixed at 1.2 except for MnF_2 (2.7 probably because of some instability of the experiment). Lorentzian width (FWHM in eV) is 2.2 for MnF_2 , 2.1 for MnCl_2 and for MnBr_2 (fixed).

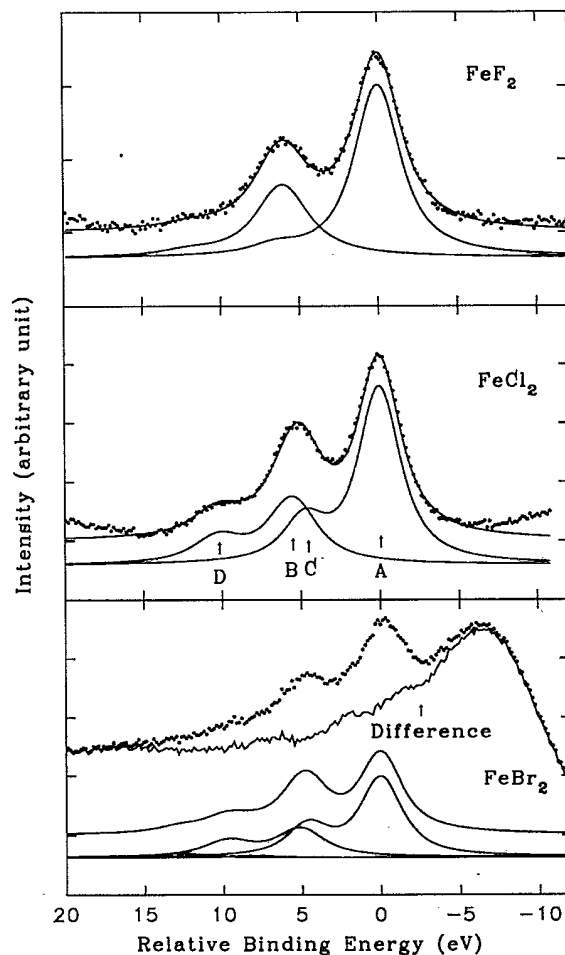


FIG. 4. The 3s spectra of Fe dihalides. Inelastic background and x-ray source satellites were subtracted from the raw data, except for the case of FeBr_2 where only x-ray source satellites were subtracted. Fitting curves and their components are shown. Gaussian width (FWHM in eV) was fixed at 1.2. Lorentzian width (FWHM in eV) is 3.1 (high spin) and 3.7 (low spin) for FeF_2 , 2.7 (high spin) and 3.4 (low spin) for FeCl_2 and for FeBr_2 (fixed).

TABLE II. The ligand-hole d -electron Coulomb attraction u estimated from cation-anion distance R from Ref. 22 and electronic dielectric constant ϵ_∞ . ϵ_∞ was calculated from the Clausius-Mossotti relation using reported values of polarizability (Refs. 25 and 26).

	R (Å)	ϵ_∞ (Å ⁻³)	u (eV)
MnF ₂	2.1	2.1	3.3
MnCl ₂	2.6	3.0	1.8
MnBr ₂	2.7	4.7	1.1
FeF ₂	2.0	3.0	2.4
FeCl ₂	2.5	3.6	1.6
FeBr ₂	2.7	4.9	1.1
MnO	2.2	4.9	1.3
FeO	2.2	5.9	1.1

comes from the observation that this coupling strength is essentially the sum of two electron matrix elements between $3p^2$ and $3s3d$ and that if the d -electron vacancies are small, then there will be fewer of these matrix elements. By a crude estimate, for which we treat $3p^2$ just like the ligand hole in the charge-transfer model, we could find that this decrease of the coupling strength behaves as $\sim \sqrt{(10-n+q)}/\sqrt{(10-n)}$. If we consider this behavior of the intrashell correlation effect coupling strength, we get Q_L smaller than Q_H by ~ 3 eV and $Q_L \approx Q_{2p}$. We feel that this is the main cause of the deviation of the separation between Q_L and Q_H from the atomic estimation.

In the case of MnBr₂ and FeBr₂, the loss structure from Br $3d$ is quite large, and it is impossible to separate out $3s$ structures. So we calculated the expected $3s$ spectra using the parameter values obtained above, and show it in the figure along with the difference curve from the actual spectra. We see that the bumps in the experimental data all correspond to the theoretical peaks quite well, and the resultant difference curve is very smooth as expected of the loss structure. Furthermore, for MnBr₂ the position of the maximum height of the resulting difference curve turned out to be 17.1 eV away from the Br $3d$ peak position. This is nearly equal to the energy difference between the Br $3p$ peak and its loss structure, which was found to be 17.4 eV. Hence, we conclude that our model explains very well both the $2p$ and $3s$ core-level spectra of all Mn and Fe dihalide compounds studied here consistently.

C. $2p_{3/2}$ and $3s$ spectra of mono-oxides

In Figs. 5 and 6 we show the $2p_{3/2}$ and $3s$ spectra of FeO and MnO and their fitted curves in the same way as in Figs. 1–4. FeO $2p$ and $3s$ spectra were taken in our laboratory^{18,27} with the Al $K\alpha$ photon source. MnO $2p$ and $3s$ spectra were taken from the work of Hermsmeier *et al.*²⁸ We used their data taken at an angle $\theta=90^\circ$, $\phi=0^\circ$ with the Al $K\alpha$ photon source. We fitted the $2p$ spectra as usual and obtained the charge-transfer model parameter values $\Delta=7.4$ eV, $U=3.2$ eV, $T=1.5$ eV, $Q_{2p}=4.6$ eV for MnO, and 6.5, 3.9, 1.5, and 5.6 eV, respectively, for FeO. We see that the U , T , and Q values

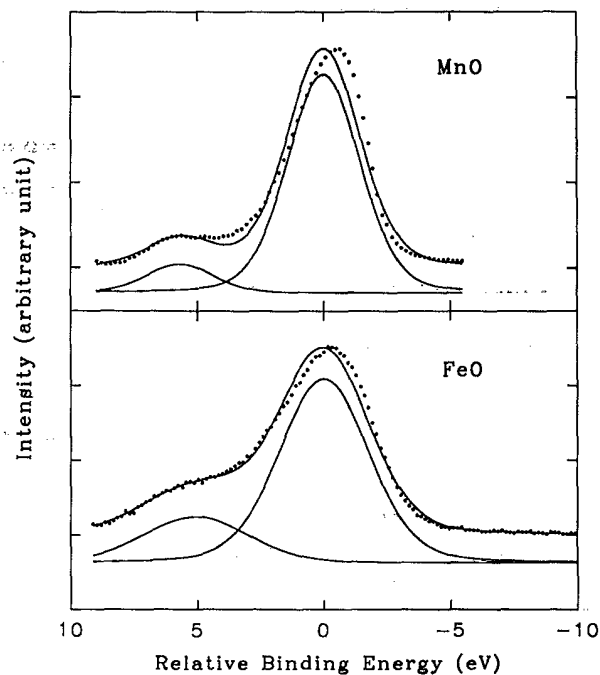


FIG. 5. The $2p_{3/2}$ spectra of MnO and FeO. Lorentzian widths were fixed at the same values as the dihalide cases. Gaussian widths (FWHM in eV) are 3.0 (main), 2.8 (satellite) for MnO and 3.7 (main), 4.4 (satellite) for FeO.

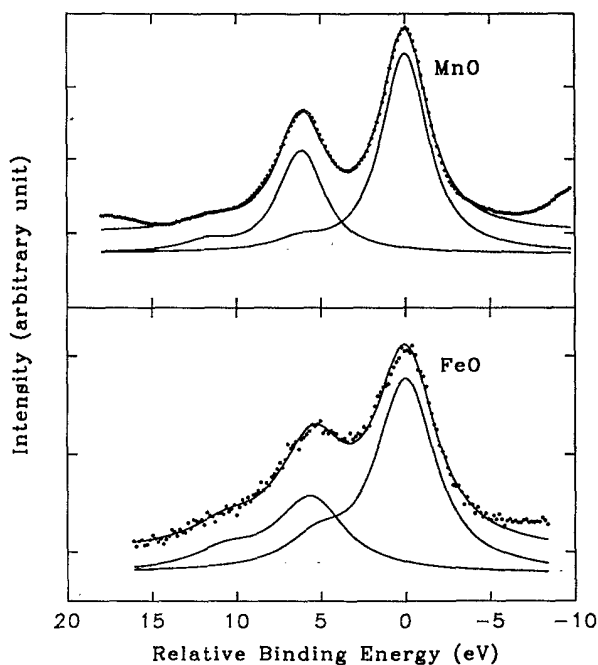


FIG. 6. The $3s$ spectra of MnO and FeO. Gaussian width (FWHM in eV) is 1.1 for MnO and 1.2 for FeO. Lorentzian width (FWHM in eV) is 2.9 for MnO, 3.8 (high spin) and 4.6 (low spin) for FeO. The ratio of Lorentzian widths between the high-spin and the low-spin peak was constrained to be equal to that of difluorides and dichlorides.

are slightly different from those of dihalides. Now we fitted the 3s spectra in the same way as for dihalides. We find in these figures that these spectra are fitted quite well with our model as in the case of dihalides. The parameter values for these fittings are listed in the bottom rows of Table I. The u values were calculated in the point-charge approximation as before with the physical parameter values^{18,25} listed in Table II. The character of the spectra for these mono-oxides is found to be halfway between fluorides and chlorides but it is closer to the chloride character. To sum up, we conclude that the 2p and 3s spectra of MnO and FeO are also explained very well, and consistently, in our model.

V. FINAL-STATE SCREENING EFFECT IN THE 3s PHOTOEMISSION

To understand the nature of each peak in the 3s spectra, we calculated the final eigenstate corresponding to each peak. The results are listed in Table III. The peaks labeled *A* and *C* originate from the high-spin states, and peaks *B* and *D* from the low-spin final states. Peaks *A* and *B* are main peaks for each spin final state, and peaks *C* and *D* can be called charge-transfer satellites. We see that the second peak in the raw spectrum, which has been considered to be an exchange-split multiplet peak, actually consists of two contributions *B* and *C*. For fluorides,

TABLE III. Relative energy (in units of eV), intensity, and state vectors of theoretical peaks comprising the 3s spectra of Mn and Fe dihalides and mono-oxides. In expressing state vectors the numbers shown are the squares of the coefficients. The components for configurations with more than two (one for states with two 3p holes) ligand holes are not shown because their intensities are usually very small.

Compound	Peak	Spin state	Position	Intensity	State vector				
					sd^n	$sd^{n+1}\underline{L}$	$sd^{n+2}\underline{L}^2$	p^2d^{n+1}	$p^2d^{n+2}\underline{L}$
MnF ₂	<i>A</i>	⁷ S	0	1.0	0.85	0.14	0.01		
	<i>B</i>	⁵ S	6.5	0.53	0.62	0.12	0.11	0.21	0.03
	<i>C</i>	⁷ S	7.8	0.01	0.15	0.74	0.11		
	<i>D</i>	⁵ S	13.6	0.01	0.12	0.56	0.10	0.05	0.15
MnCl ₂	<i>A</i>	⁷ S	0	1.0	0.54	0.40	0.06		
	<i>B</i>	⁵ S	6.0	0.50	0.32	0.36	0.07	0.11	0.11
	<i>C</i>	⁷ S	5.0	0.09	0.43	0.33	0.23		
	<i>D</i>	⁵ S	10.7	0.09	0.38	0.15	0.21	0.13	0.04
MnBr ₂	<i>A</i>	⁷ S	0	1.0	0.34	0.52	0.13		
	<i>B</i>	⁵ S	5.6	0.45	0.15	0.4	0.17	0.05	0.13
	<i>C</i>	⁷ S	4.4	0.19	0.57	0.09	0.30		
	<i>D</i>	⁵ S	10.0	0.17	0.42	0.00	0.27	0.15	0.00
FeF ₂	<i>A</i>	⁶ D	0	1.0	0.75	0.23	0.01		
	<i>B</i>	⁴ D	6.0	0.50	0.54	0.21	0.02	0.17	0.06
	<i>C</i>	⁶ D	6.5	0.05	0.24	0.62	0.13		
	<i>D</i>	⁴ D	12.0	0.03	0.20	0.45	0.12	0.07	0.12
FeCl ₂	<i>A</i>	⁶ D	0	1.0	0.39	0.51	0.10		
	<i>B</i>	⁴ D	5.5	0.45	0.21	0.44	0.11	0.07	0.13
	<i>C</i>	⁶ D	4.8	0.23	0.55	0.18	0.25		
	<i>D</i>	⁴ D	10.3	0.17	0.45	0.05	0.24	0.15	0.01
FeBr ₂	<i>A</i>	⁶ D	0	1.0	0.22	0.58	0.19		
	<i>B</i>	⁴ D	5.1	0.42	0.10	0.44	0.22	0.03	0.13
	<i>C</i>	⁶ D	4.6	0.38	0.59	0.01	0.35		
	<i>D</i>	⁴ D	9.7	0.24	0.34	0.03	0.32	0.11	0.01
MnO	<i>A</i>	⁷ S	0	1.0	0.66	0.30	0.03		
	<i>B</i>	⁵ S	6.1	0.51	0.43	0.29	0.04	0.14	0.09
	<i>C</i>	⁷ S	6.3	0.05	0.32	0.46	0.21		
	<i>D</i>	⁵ S	11.8	0.05	0.29	0.26	0.19	0.11	0.08
FeO	<i>A</i>	⁶ D	0	1.0	0.52	0.42	0.06		
	<i>B</i>	⁴ D	5.6	0.46	0.31	0.39	0.07	0.10	0.12
	<i>C</i>	⁶ D	5.2	0.14	0.45	0.32	0.22		
	<i>D</i>	⁴ D	10.6	0.12	0.40	0.14	0.20	0.14	0.04

however, peak C (and peak D) is very weak, and peaks A and B are mainly of "unscreened" d^n character. In this case, we found practically no change of calculated spectra whether we include the charge-transfer effect or not. So, we can say that the final-state screening effect is very weak here and the observed energy splitting in the 3s spectrum is the exchange splitting of the $3s3d^n$ configuration, as in the original interpretation of Fadley *et al.*¹ However, we expect that care must be taken for other transition-metal fluorides because the screening effect becomes stronger for heavier metal ions such as Co^{2+} or Ni^{2+} . When we examine the spectra reported in the literature,³ this is obvious for CoF_2 and is very likely for NiF_2 where it seems that C-like and D-like peaks are nontrivial but are strongly mixed with A-like and B-like peaks into one slightly structured asymmetric peak. For dichlorides, we see that the state vectors of peaks A and B have such a strongly mixed character between the unscreened state and locally screened state that we cannot say one of these two is dominant over the other. In dibromides, however, the "locally screened" configuration dominates both peak A and peak B, and peaks C and D are due to the "unscreened" $3s3d^n$ state. In monoxides, the characters of peaks are between fluorides and chlorides, although somewhat closer to chlorides. We see that the importance of screening depends on the ligand, and it is too simple minded to assign "screened" or "unscreened" peaks for all compounds.

Therefore, because of the screening effect in the final state, we cannot in general rely on the simple multiplet theory (including intrashell correlation effect) to interpret the experimental 3s energy splittings. Each peak in the spectrum does not originate from a well-defined multiplet configuration. Instead, it must be borne in mind that in each peak there are contributions from the configuration having extra-atomic electrons transferred from the ligand. Moreover, the purity of the spin state in the second peak in the raw spectra cannot be guaranteed since it is actually a superposition of the low-spin main peak and the high-spin charge-transfer satellite. The observed peak position is therefore the weighted average of the low-spin peak B and the high-spin peak C energy positions, although it is very close to (only 0.2–0.4 eV smaller) the position of peak B as can be deduced from Table III. A more important effect, which is responsible for the observed trend in the change of the measured splittings depending on the compounds along the series

for a given Mn^{2+} or Fe^{2+} , is that the energy of peak B is much affected by the final-state screening. Compared to fluorides, the energy splitting between peak A and peak B decreases by 0.5–1.1 eV for chlorides and bromides, which is comparable to the difference of hybridization shifts 0.7–1.2 eV between high-spin and low-spin final

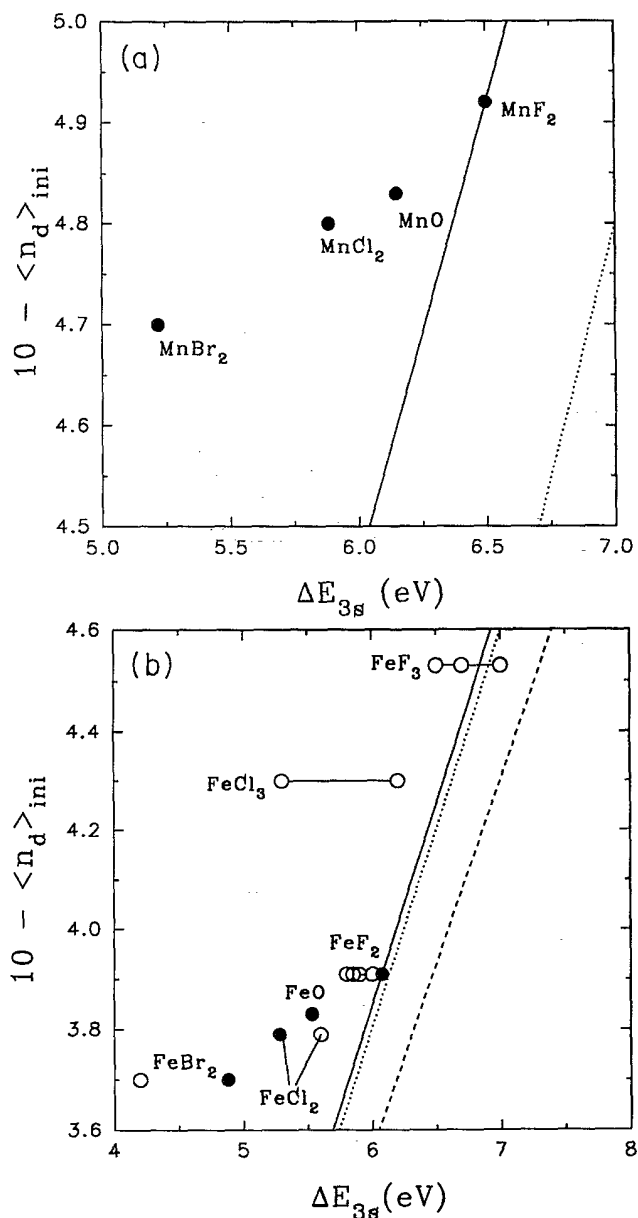


TABLE IV. The comparison of cation local magnetic moments [(In Bohr magnetons) (Refs. 26–28)] with the values of $10 - \langle n_d \rangle_{\text{ini}}$ shown in Table I for Mn and Fe dihalides.

	Cation moment	$10 - \langle n_d \rangle_{\text{ini}}$	Difference
MnF_2	4.98	4.92	0.06
MnCl_2	4.84	4.80	0.04
MnBr_2		4.7	
FeF_2	4.64	3.91	0.73
FeCl_2	4.5	3.79	0.71
FeBr_2	4.4	3.70	0.70

FIG. 7. (a) 3s energy splittings vs $10 - \langle n_d \rangle_{\text{ini}}$ for Mn^{2+} insulating compounds. The solid line is the empirical Van Vleck theorem line with the value of $G^2(3s,3d)$ obtained from the MnF_2 data. If we use half the multiplet-hole theory value of $G^2(3s,3d)$, then we get the dotted line for Mn^{2+} . (b) 3s energy splittings vs $10 - \langle n_d \rangle_{\text{ini}}$ for Fe^{2+} insulating compounds. We also included the data of Acker *et al.* (Ref. 6) data for Fe dihalides and trihalides. Their data are shown with open circles, while ours are marked with filled circles. The solid line is the empirical Van Vleck theorem line with the value of $G^2(3s,3d)$ obtained from the FeF_2 data. If we use half the multiplet-hole theory value of $G^2(3s,3d)$, then we get the dotted line for Fe^{2+} and the dashed line for Fe^{3+} , respectively.

states due to the charge transfer alone for chlorides and bromides. This difference of hybridization shifts comes about because different Q values depending upon the spin (Q_H and Q_L) give rise to different amounts of final-state screening and this effect increases as Δ decreases.

Now let us comment on the controversial problem about the correlation between the local magnetic moment and the $3s$ energy splitting measured in the photoemission. First, we note that the local magnetic moment can differ from the spin magnetic moment in the ground state due to the unquenched orbital angular-momentum contribution to the magnetic moment.²⁶ In our scheme, the quantity which can be interpreted as the spin magnetic moment of the localized d shell in the ground state will be $10 - \langle n_d \rangle_{\text{ini}}$, where $\langle n_d \rangle_{\text{ini}}$ is the number of d electrons in the ground state. The values of $\langle n_d \rangle_{\text{ini}}$ calculated in our analyses are listed in Table I. In Table IV we compare reported values of magnetic moments with our estimated spin magnetic moments for dihalides. Magnetic moments for MnF_2 and FeF_2 are from Ref. 29 (neutron diffraction), for MnCl_2 from Ref. 30, and for FeCl_2 and FeBr_2 from Ref. 31 (neutron diffraction). We see that the difference is nearly zero for MnF_2 and MnCl_2 and about 0.7 Bohr magnetons for Fe dihalides. Thus, for Mn^{2+} there is no orbital contribution to the magnetic moment as must be the case, and for Fe^{2+} the observed magnetic moments contain a substantial amount of orbital angular-momentum contributions which are nearly constant along the series. So, we observe that $10 - \langle n_d \rangle_{\text{ini}}$ obtained by the core-level analysis using the charge-transfer model is a reasonable estimate of the spin magnetic moment. If we want to ask the relationship between the $3s$ splitting and the local spin magnetic moment, it will be proper to compare this quantity $10 - \langle n_d \rangle_{\text{ini}}$ or its equivalent corrected from the experimental value with the $3s$ splitting. We show in Fig. 7 the measured $3s$ energy splittings versus $10 - \langle n_d \rangle_{\text{ini}}$ along with the Van Vleck theorem lines using the Slater exchange integral determined from the data of MnF_2 and FeF_2 . Also shown are the curves with the Slater exchange integral fixed at half the multiplet-hole theory value, for comparison. The data of Acker *et al.*⁶ for Fe

dihalides and trihalides are also included in the figure. We note that the empirical Van Vleck line is the same kind as the calibration curve proposed by Kowalczyk *et al.*,¹² since they draw their line by using FeF_2 and FeF_3 data, although the actual magnetic moment of FeF_3 is smaller than the purely ionic value they assumed. We can observe in this Fig. 7 the trends mentioned above, i.e., as the compound becomes more covalent then the measured splitting becomes smaller and smaller than the empirical Van Vleck curve.

VI. SUMMARY

We were able to understand the $3s$ core-level photoemission spectra of Mn and Fe dihalides and mono-oxides systematically by a combination of exchange interaction, intrashell electron correlation effect, and charge-transfer final-state screening mechanism. We were able to do this consistently with the interpretation of $2p$ spectra. For MnF_2 and FeF_2 , $3s$ energy splittings are determined mainly by the exchange interaction between $3s$ hole and the localized $3d$ electrons in the ground state. However, as the ligand electronegativity decreases the charge-transfer satellites become important, and the peaks in the $3s$ spectra lose its purity of spin states. In this case, the observed energy splitting does not reflect the magnetic moment either in the "unscreened" ($3d^n$) state or in the "screened" ($3d^{n+1}$) state, and must be interpreted with a full consideration of intrashell correlation effect and charge-transfer mechanism. These effects prevent the simple exchange-splitting interpretation of the $3s$ spectra. The values and trend of $3s$ energy splittings observed as the compound gets more covalent are explained by the different amount of screening depending upon the spin of the final state of photoemission. And this makes the observed peak splittings smaller than those expected from, say, simple Van Vleck theorem.

ACKNOWLEDGMENT

This work was supported in part by a grant from the Ministry of Education, Korea.

¹C. S. Fadley, D. A. Shirley, A. J. Freeman, P. S. Bagus, and J. V. Mallow, *Phys. Rev. Lett.* **23**, 1397 (1969); C. S. Fadley and D. A. Shirley, *Phys. Rev. A* **2**, 1109 (1970).

²P. S. Bagus, A. J. Freeman, and F. Sasaki, *Phys. Rev. Lett.* **30**, 850 (1973).

³B. W. Veal and A. P. Paulikas, *Phys. Rev. Lett.* **51**, 1995 (1983); B. W. Veal and A. P. Paulikas, *Phys. Rev. B* **31**, 5399 (1985).

⁴B. Sinkovic *et al.*, *Phys. Rev. Lett.* **55**, 1227 (1985); B. Hermsmeier *et al.*, *ibid.* **62**, 478 (1989).

⁵B. Hermsmeier, C. S. Fadley, M. O. Krause, J. Jimenez-Mier, P. Gerard, and S. T. Manson, *Phys. Rev. Lett.* **61**, 2592 (1988).

⁶J. F. van Acker, Z. M. Stadnik, J. C. Fuggle, H. J. W. M. Hoekstra, K. H. J. Buschow, and G. Stroink, *Phys. Rev. B* **37**,

6827 (1988).

⁷F. U. Hillebrecht *et al.*, *Phys. Rev. Lett.* **65**, 2450 (1990).

⁸J. H. Van Vleck, *Phys. Rev.* **45**, 405 (1934).

⁹S. P. Kowalczyk, L. Ley, R. A. Pollak, F. R. McFeely, and D. A. Shirley, *Phys. Rev. B* **7**, 4009 (1973).

¹⁰D. A. Shirley, in *Photoemission in Solids I*, edited by M. Cardona and L. Ley (Springer-Verlag, New York, 1978), Chap. 4.

¹¹Eeva-Kaarina Viinikka and Yngve Öhrn, *Phys. Rev. B* **11**, 4168 (1975).

¹²S. P. Kowalczyk, F. R. McFeely, L. Ley, and D. A. Shirley, in *Magnetism and Magnetic Materials*, edited by C. D. Graham *et al.* (AIP, New York, 1975), p. 207.

¹³J. Azoulay and L. Ley, *Solid State Commun.* **31**, 131 (1979).

¹⁴D. J. Joyner, O. Johnson, and D. M. Hercules, *J. Phys. F* **10**, 169 (1980).

- ¹⁵G. van der Laan, C. Westra, C. Haas, and G. A. Sawatzky, *Phys. Rev. B* **23**, 4369 (1981).
- ¹⁶J. Zaanen, C. Westra, and G. A. Sawatzky, *Phys. Rev. B* **33**, 8060 (1986).
- ¹⁷Jaehoon Park, Seungoh Ryu, Moon-sup Han, and S-J. Oh, *Phys. Rev. B* **37**, 10 867 (1988).
- ¹⁸Geunseop Lee and S.-J. Oh, *Phys. Rev. B* **43**, 14 674 (1991).
- ¹⁹J. Zaanen, G. A. Sawatzky, and J. W. Allen, *Phys. Rev. Lett.* **55**, 418 (1985).
- ²⁰V. Kinsinger, I. Sander, P. Steiner, R. Zimmermann, and S. Hufner, *Solid State Commun.* **73**, 527 (1990).
- ²¹S.-J. Oh, Gey-Hong Gweon, and Je-Geun Park, *Phys. Rev. Lett.* **68**, 2850 (1992).
- ²²Ralph W. G. Wyckoff, *Crystal Structures*, 2nd ed. (Interscience, New York, 1963), Vol. 1.
- ²³S. P. Kowalczyk, L. Ley, F. R. McFeely, and D. A. Shirley, *Phys. Rev. B* **11**, 1721 (1975); R. P. Gupta and S. K. Sen, *ibid.* **B 10**, 71 (1974).
- ²⁴B. W. Veal, D. E. Ellis, and D. J. Lam, *Phys. Rev. B* **32**, 5391 (1985).
- ²⁵J. Shanker, H. P. Sharma, and B. R. K. Gupta, *Solid State Commun.* **21**, 903 (1977).
- ²⁶Ashcroft and Mermin, *Solid State Physics* (Holt, Rinehart and Winston, New York, 1976).
- ²⁷Geunseop Lee (unpublished).
- ²⁸B. Hermsmeier, J. Osterwalder, D. J. Friedman, B. Sinkovic, T. Tran, and C. S. Fadley, *Phys. Rev. B* **42**, 11 895 (1990).
- ²⁹R. A. Erickson, *Phys. Rev.* **90**, 779 (1953).
- ³⁰Linus Pauling, *The Nature of the Chemical Bond*, 3rd. ed. (Cornell University Press, New York, 1960).
- ³¹M. K. Wilkinson, J. W. Cable, E. O. Wollan, and W. C. Koehler, *Phys. Rev.* **113**, 497 (1959).